



Crucial Role of ppGpp in the Resilience of *Escherichia coli* to Growth Disruption

Clément Patacq,^{a,b} Nicolas Chaudet,^b  Fabien Létisse^a

^aTBI, Université de Toulouse, INSA, INRAE, CNRS, UPS, Toulouse, France

^bSanofi Pasteur, Département de Bioprocédés R&D, Marcy-l'Etoile, France

ABSTRACT Bacteria grow in constantly changing environments that can suddenly become completely depleted of essential nutrients. The stringent response, a rewiring of the cellular metabolism mediated by the alarmone (p)ppGpp, plays a crucial role in adjusting bacterial growth to the severity of the nutritional stress. The ability of (p)ppGpp to trigger a slowdown of cell growth or induce bacterial dormancy has been widely investigated. However, little is known about the role of (p)ppGpp in promoting growth recovery after severe growth inhibition. In this study, we performed a time-resolved analysis of (p)ppGpp metabolism in *Escherichia coli* as it recovered from a sudden slowdown in growth. The results show that *E. coli* recovers by itself from the growth disruption provoked by the addition of serine hydroxamate, the serine analogue that we used to induce the stringent response. Growth inhibition was accompanied by a severe disturbance of metabolic activity and, more surprisingly, a transient overflow of valine and alanine. Our data also show that ppGpp is crucial for growth recovery since in the absence of ppGpp, *E. coli*'s growth recovery was slower. In contrast, an increased concentration of pppGpp was found to have no significant effect on growth recovery. Interestingly, the observed decrease in intracellular ppGpp levels in the recovery phase correlated with bacterial growth, and the main effect involved in the return to the basal level was identified by flux calculation as growth dilution. This report thus significantly expands our knowledge of (p)ppGpp metabolism in *E. coli* physiology.

IMPORTANCE The capacity of microbes to resist and overcome environmental insults, known as resilience, allows them to survive in changing environments but also to resist antibiotic and biocide treatments and immune system responses. Although the role of the stringent response in bacterial resilience to nutritional stresses has been well studied, little is known about its importance in the ability of the bacteria to not just resist but also recover from these disturbances. To address this important question, we investigated growth disruption resilience in the model bacterium *Escherichia coli* and its dependence on the stringent response alarmone (p)ppGpp by quantifying ppGpp and pppGpp levels as growth was disrupted and then recovered. Our findings may thus contribute to understanding how ppGpp improves *E. coli*'s resilience to nutritional stress and other environmental insults.

KEYWORDS *Escherichia coli*, metabolic adaptation, metabolic regulation, stringent response

As single-cell organisms, bacteria face constant changes in their direct physico-chemical and nutritional environments. To overcome these disturbances, bacteria have developed adaptive properties that allow them to survive, grow, and eventually evolve. Depletion of external nutrients is one of the most serious insults for these organisms because they have very little internal storage, and their ability to rapidly modulate metabolic functions is key to their survival. A central component of this

Citation Patacq C, Chaudet N, Létisse F. 2020. Crucial role of ppGpp in the resilience of *Escherichia coli* to growth disruption. *mSphere* 5:e01132-20. <https://doi.org/10.1128/mSphere.01132-20>.

Editor Gary Sawers, Martin Luther University of Halle-Wittenberg Institute of Biology/Microbiology

Copyright © 2020 Patacq et al. This is an open-access article distributed under the terms of the [Creative Commons Attribution 4.0 International license](https://creativecommons.org/licenses/by/4.0/).

Address correspondence to Fabien Létisse, fabien.letisse@insa-toulouse.fr.

Received 6 November 2020

Accepted 25 November 2020

Published 23 December 2020

metabolic adaptation to nutrient stress is the stringent response, a pleiotropic mechanism in bacteria that coordinates growth and nutrient availability (1) and affects a wide range of cellular processes (2). The stringent response is mediated by the accumulation of guanosine tetra- and pentaphosphates [guanosine 3',5'-bis(diphosphate) and guanosine 3'-diphosphate,5'-triphosphate], collectively known as (p)ppGpp, which act as second messengers to fundamentally reprogram cellular physiology from rapid growth in rich nutritional environments to survival and adaptation when nutrients become scarce (3, 4). (p)ppGpp also plays other important roles in the regulation of bacterial virulence (5), survival during host invasion (6), and antibiotic resistance and persistence (7–9). Intracellular levels of (p)ppGpp are controlled by RSH (RelA-SpoT homologue) enzymes (10), whose name derives from the (p)ppGpp synthetase RelA and the (p)ppGpp synthetase/hydrolase SpoT in *Escherichia coli*, where (p)ppGpp was originally detected (11).

For this bacterium, it has been established for decades that the reaction to amino acid limitation is a RelA-mediated stringent response (3). RelA is a GDP/GTP pyrophosphokinase that, depending on whether the substrate is GDP or GTP, catalyzes the formation of ppGpp or pppGpp via a ribosome-associated mechanism (12, 13). SpoT-mediated stringent responses occur under other nutritional stresses such as fatty acid starvation (14), carbon source starvation (15), phosphorus limitation (16, 17), and iron limitation (18). In the case of carbon source diauxic growth transitions, there is evidence that both RelA- and SpoT-mediated responses are involved (19). (p)ppGpp, the alarmone that these enzymes synthesize, acts globally, directly and indirectly, on replication, transcription, translation (20), and protein activities (21, 22). In addition to RelA and SpoT, the pppGpp pyrophosphatase GppA also modulates intracellular levels of (p)ppGpp by converting pppGpp into ppGpp. To date, the physiological role of pppGpp remains unclear as it has been shown to be a less potent regulator than ppGpp (21, 23, 24).

It is well established that basal levels of (p)ppGpp control growth by modulating the number of ribosomes (3, 25). The sudden accumulation of (p)ppGpp provokes a quasi-immediate inhibition of growth (26) and protein synthesis (27, 28). The nature (transient and reversible) and the potency of (p)ppGpp interactions with ribosome-associated GTPases may explain how (p)ppGpp buildup contributes to slowing down growth and reduces translational activity (21). Remarkably, the ability of bacterial cells faced with nutritional stress to resume growth and recover the predisturbance rate and the role of (p)ppGpp in promoting this resilience have not been systematically studied.

In this study, therefore, we investigated (i) the ability of *E. coli* to cope with severe growth inhibition and (ii) the contribution of (p)ppGpp metabolism to *E. coli*'s capacity to adapt to disruptions such as these. We triggered a stringent response using serine hydroxamate (SHX), a serine analogue known to have this effect on *E. coli* (11). SHX addition promotes (p)ppGpp accumulation and provokes growth arrest (29, 30) because of presumed competitive inhibition with serine binding to seryl-tRNA synthetase (29, 31), along with other inhibitory effects on cellular component synthesis, notably on phospholipid synthesis (32). The response to SHX-induced homeostasis disruption was dissected by analyzing growth rate dynamics and quantifying the intracellular levels of ppGpp and pppGpp in perturbation experiments using the wild-type (WT) K-12 strain of *E. coli* and $\Delta relA$ and $\Delta gppA$ mutants. Our results provide clear evidence of the resilience of *E. coli* to growth disruption caused by SHX addition and demonstrate the key role played by ppGpp, and not by pppGpp, in *E. coli*'s ability to recover its full growth capacity.

RESULTS

Dynamic response to SHX addition. The macroscopic effects of SHX addition were characterized in *Escherichia coli* K-12 MG1655 cells growing exponentially in minimal medium with 110 mM glucose (20 g · liter⁻¹) as the sole carbon source. Growth was

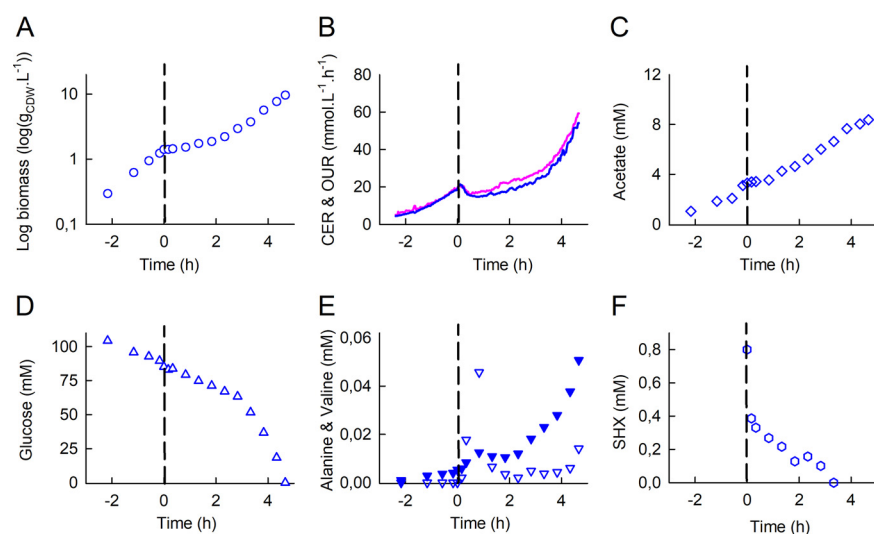


FIG 1 Dynamics of the response of *E. coli* K-12 MG1655 to SHX addition during exponential growth in a bioreactor: time evolutions of biomass (A), the oxygen uptake rate (OUR) (pink) and the carbon dioxide evolution rate (CER) (blue) (B), the acetate concentration (C), the glucose concentration (D), alanine (downward triangles) and valine (filled downward triangles) concentrations (E), and the SHX concentration (F). Time zero was defined as the moment when SHX (0.8 mM) was added to the bioreactor. The OUR and CER were determined from online measurements of O_2 , CO_2 , and N_2 percentages as described in Materials and Methods. Biomass and extracellular metabolite concentrations were measured in culture samples collected every 10 min to 1 h. The data are highly reproducible (see Fig. S1 in the supplemental material).

performed aerobically under controlled conditions in bioreactors. SHX (0.8 mM) was added when the optical density (OD) reached 3.5.

As expected, adding SHX immediately led to severe growth inhibition (Fig. 1A), with concomitant decreases in the OUR (oxygen uptake rate) and CER (carbon dioxide evolution rate) (Fig. 1B), indicating a strong decrease in respiratory activity. Combined with the interruption of acetate production (Fig. 1C) and, to a lesser extent, glucose consumption (Fig. 1D), these events reflect a sharp reduction in metabolic activity. However, the inhibition of growth and reduction in metabolic activity were transient, and about 1.5 h after SHX addition, the biomass concentration, respiratory activity, and acetate production began to increase once again (Fig. 1A).

During the exponential growth phase, we detected relatively low levels (micromolar range) of alanine and valine in the culture medium (Fig. 1E), along with other metabolic by-products (rostate and dihydroorotate) (data not shown) and traces of leucine (data not shown). Interestingly, SHX addition led to sharp increases in the concentrations of alanine and valine, which were about 8 times and 2 times higher, respectively, 20 min after than just before SHX addition and peaked 50 min after SHX addition (at 20 times and 3 times their pre-SHX levels, respectively). In this period, the estimated fluxes of alanine and valine excretion were 9% and 2%, respectively, of the fluxes required to support growth during the exponential phase (see Table S1 in the supplemental material). The alanine and valine concentrations in the medium then dropped and finally increased once again as growth resumed as it was before SHX addition.

Surprisingly, we observed that the SHX concentration in the cultivation medium decreased immediately after it was added, becoming undetectable after 2.8 h (Fig. 1F). The disappearance of SHX is biotic in origin since the SHX concentration did not decrease under similar conditions but without cells (Fig. S2). In addition, nuclear magnetic resonance (NMR) did not detect any SHX degradation products. To our knowledge, this has never previously been reported in the literature despite SHX being widely used to trigger the stringent response.

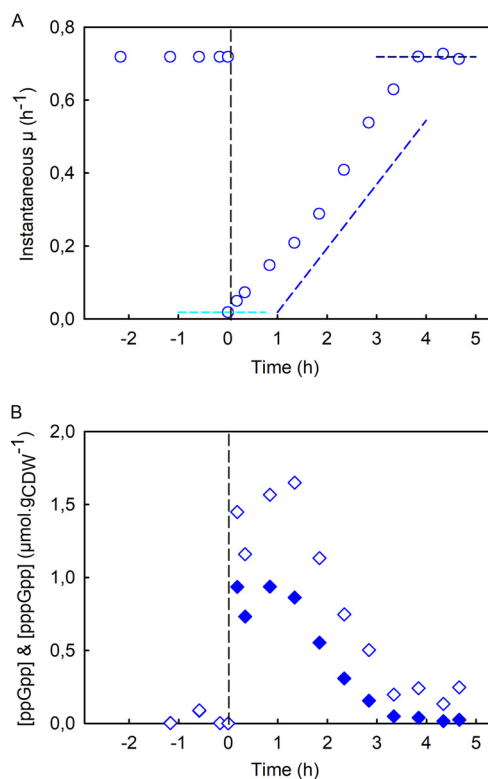


FIG 2 Resilience of *E. coli* K-12 MG1655 to growth disruption. (A) Instantaneous growth rate, $\mu_{(t)}$ (blue circles), as a function of time before and after SHX addition. The cyan dashed line indicates the robustness parameter, the slope of the blue dashed line is the recovery rate, and the dark blue dashed line represents the recovered steady state. The values of these parameters are given in Table 1. (B) Intracellular concentrations of ppGpp (diamonds) and pppGpp (filled diamonds) (micromoles per gram of cell dry weight) before and after the addition of SHX. The data are highly reproducible (see Fig. S3 in the supplemental material).

***Escherichia coli* is resilient to SHX addition.** Although the addition of SHX profoundly perturbs its metabolism, these results reveal that *E. coli* recovers its growth capacity, at least partially. To better characterize *E. coli*'s resilience to SHX addition, we calculated the instantaneous growth rate throughout the experiment (Fig. 2A). The growth rate before SHX addition was $0.71 \pm 0.01 \text{ h}^{-1}$ (Fig. S4A), in agreement with previously reported data on *E. coli* K-12 growing in minimal medium (33, 34). The growth rate decreased suddenly down to near zero after SHX was added, before increasing constantly and leveling off about 4 h after SHX addition at a value similar to the one measured before SHX addition. Interestingly, the growth profiles measured here are typical of those of resilience-engineered systems able to recover their initial performance levels after disruptive events (35, 36). Here, growth is the biological property that *E. coli* is able to recover. In keeping with the concept of resilience engineering, we defined three metrics to describe the resilience of *E. coli* to the disruptions caused by SHX addition: (i) robustness, defined here as the residual growth rate after SHX addition; (ii) the recovery rate, which is the recovery profile of the growth rate (assumed here to be linear); and (iii) the recovered steady state, which corresponds here to the growth rate at the end of the recovery process (expressed relative to the initial growth rate). These metrics are represented by dashed lines in Fig. 2A, and the corresponding numerical values are given in Table 1.

Dynamics of intracellular (p)ppGpp levels. The intracellular concentrations of ppGpp and pppGpp were measured throughout the experiment by liquid chromatography-tandem mass spectrometry (LC-MS/MS) (37) (Fig. 2B). As expected, the addition of SHX led to a sudden intracellular accumulation of ppGpp, whose concentration was

TABLE 1 Metrics used to quantify the resilience of *E. coli* to SHX-induced growth disruption^a

Strain	Mean robustness (%) ± SD ^b	Mean recovery rate (h ⁻²) ± SD	Mean recovered steady state (%) ± SD ^b
WT	2.8 ± 2	0.1944 ± 0.0201	96.7 ± 3.3
$\Delta relA$	5.4 ± 2*	0.0847 ± 0.0261	ND
$\Delta gppA$	10.5 ± 0.5**	0.1941 ± 0.0482	98.0 ± 12.2

^aResults are presented as means ± standard deviations ($n = 3$). *, $P = 0.188$; **, $P = 0.01332$.

^bThe robustness and recovered steady state are expressed relative to the initial growth rate. ND, not determined (only one of the three biological replicates had recovered its initial growth rate 5.5 h after SHX addition).

measured to be $1.45 \mu\text{mol} \cdot (\text{g of cell dry weight})^{-1} (\text{g}_{\text{CDW}}^{-1})$ just a few minutes after SHX addition. The maximal concentration ($1.65 \mu\text{mol} \cdot \text{g}_{\text{CDW}}^{-1}$) was reached approximately 1 h after SHX addition. The ppGpp concentration then decreased continuously, tending toward the basal value measured during the exponential phase. Interestingly, the pppGpp concentration followed a similar profile albeit at lower levels; the intracellular concentration of pppGpp peaked at $0.94 \mu\text{mol} \cdot \text{g}_{\text{CDW}}^{-1}$ within 1 h of SHX addition.

Because the concentrations of both extracellular SHX and intracellular (p)ppGpp decrease during the recovery phase, it is difficult to distinguish between their respective contributions to growth recovery. Therefore, to verify that this phenomenon was associated with the stringent response and was not the result of SHX disappearing from the medium, the experiment was repeated with a $\Delta relA$ mutant. In *Bacillus subtilis*, the deletion of the counterpart gene of *relA* has been reported to suppress the accumulation of (p)ppGpp in response to SHX (38).

The stringent response is crucial for growth recovery. Before SHX addition, the growth rate of the $\Delta relA$ mutant was slightly lower than that of the wild-type strain ($0.63 \pm 0.05 \text{ h}^{-1}$) (Fig. 3A; Fig. S4A). The addition of SHX also interrupted growth and led to a reduction in metabolic activity (see the supplemental material). Note that for the $\Delta relA$ mutant, we did not measure pppGpp concentrations during the experiment, only those of ppGpp (Fig. 3B). The concentration of ppGpp in the exponential phase did not exceed $20 \pm 3 \text{ nmol} \cdot \text{g}_{\text{CDW}}^{-1}$, lower than the value measured for the WT strain ($123 \pm 85 \text{ nmol} \cdot \text{g}_{\text{CDW}}^{-1}$) (Fig. S4B) and close to the detection limit. The presence of ppGpp in this $\Delta relA$ mutant indicates that under these conditions, SpoT synthesizes low levels of ppGpp in the exponential-phase regime. As expected, we did not detect any transient accumulation of ppGpp after SHX addition. This confirms that the synthetase activity of SpoT is mainly silent in this situation and that, in agreement with previous studies (23, 27), no other RSH is involved in this response in *E. coli*. More importantly, this means that SHX addition induces growth inhibition by itself, without (p)ppGpp. Finally, although SHX disappeared completely from the medium in less than 3 h, as also observed for the WT strain (Fig. 3C), the cells had failed to fully recover their initial growth rate 6 h after SHX addition (Fig. 3A). The recovery rate of the $\Delta relA$ mutant was a factor of 2 lower ($0.0847 \pm 0.0261 \text{ h}^{-2}$) than the WT's (Table 1). These results highlight the crucial role of the stringent response in *E. coli*'s ability to overcome the growth disruption caused by SHX. Based on the analysis of instantaneous growth rates, the WT and $\Delta relA$ strains had similar robustness. Furthermore, alanine and valine were also found to accumulate in the culture medium with the $\Delta relA$ mutant, and the accumulation of alanine was even more pronounced with the mutant than it was with the WT strain (Table S1), indicating that this phenomenon is not related to the stringent response.

pppGpp overaccumulation has no effect on growth recovery. The physiological role of pppGpp in the stringent response in *E. coli* has remained unclear to date. To explore its effect on growth recovery, we applied our methodology to a mutant deleted for the *gppA* gene, which encodes the enzyme pppGpp 5'-gamma phosphohydrolase, which converts pppGpp to ppGpp. The $\Delta gppA$ mutant is known to accumulate high concentrations of pppGpp after SHX addition (23, 39).

As expected, therefore, the intracellular levels of pppGpp in the $\Delta gppA$ mutant were higher during the exponential phase than in the WT strain, while intracellular

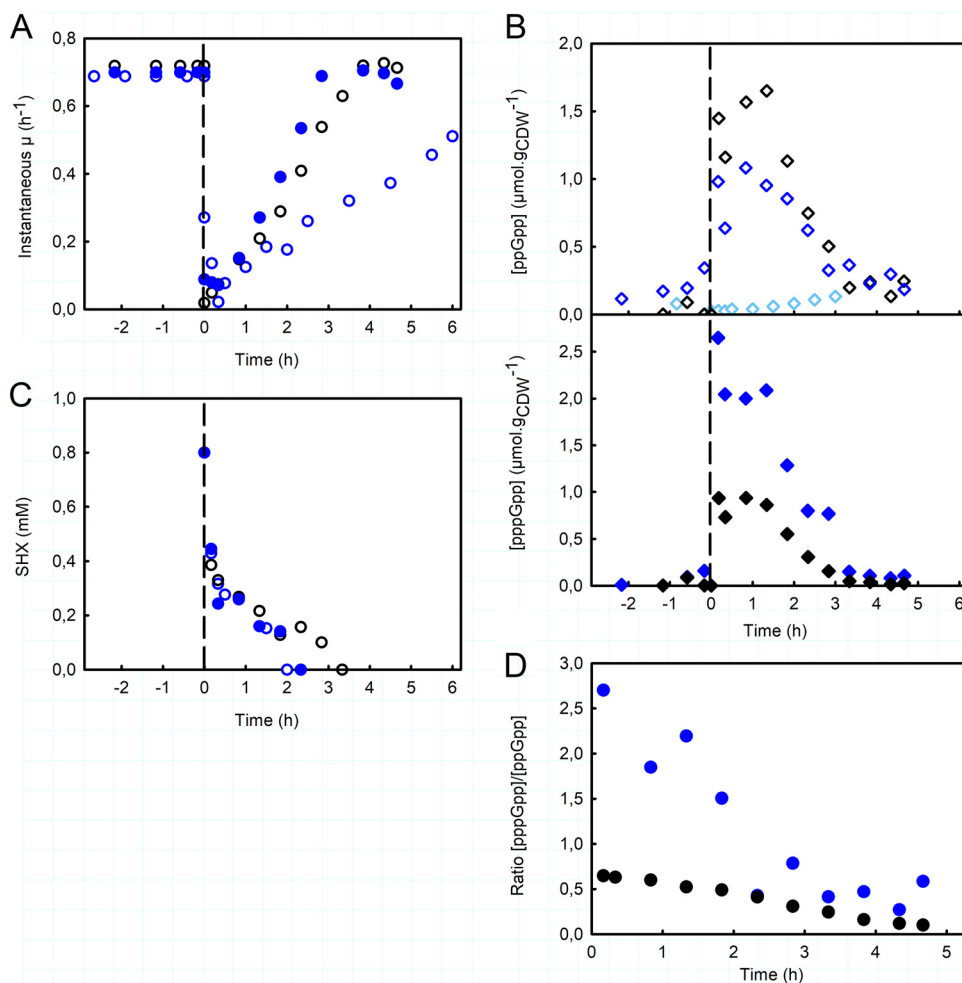


FIG 3 Importance of ppGpp for *E. coli*'s resilience. (A) Instantaneous growth rate, $\mu_{(t)}$, as a function of time before and after SHX addition, of the $\Delta relA$ mutant (blue circles), the $\Delta gppA$ mutant (filled blue circles), and the WT (black circles). (B) Intracellular concentrations of ppGpp (diamonds) and pppGpp (filled diamonds) (micromoles per gram of cell dry weight), before and after the addition of SHX, for the $\Delta relA$ mutant (light blue diamonds), the $\Delta gppA$ mutant (blue diamonds), and the WT (black diamonds). (C) Time evolution of the extracellular concentration of SHX (millimolar) for the $\Delta relA$ mutant (blue circles), the $\Delta gppA$ mutant (filled blue circles), and the WT strain (black circles). (D) Time evolution of the pppGpp/ppGpp ratio after SHX addition for the $\Delta gppA$ mutant (filled blue circles) and the WT strain (filled black circles). The corresponding results for the biological replicates are shown in Fig. S5 and S6 in the supplemental material.

ppGpp levels were similar (Fig. S4B). In the $\Delta gppA$ mutant, the concentrations of pppGpp and ppGpp were thus similar, as reported previously (24), with an estimated pppGpp/ppGpp ratio of 0.62 ± 0.38 . Although the pppGpp concentration was about 1 order of magnitude higher than that in the WT strain, the growth rates were almost identical (Fig. 3A), suggesting that pppGpp does not affect the growth rate.

As in the WT strain, the addition of SHX triggered the accumulation of ppGpp and pppGpp. However, while the ppGpp concentration varied around the same levels as those measured for the WT strain, the pppGpp concentration was roughly twice as high as that in the WT (Fig. 3B and D). The total concentration of ppGpp and pppGpp was therefore significantly higher, with the pentaphosphate form predominating, contrary to what is observed under other conditions. In this strain, the principal product of RelA is therefore pppGpp. The pppGpp/ppGpp ratio decreased over time (Fig. 3D), tending toward the value measured before SHX addition. Although this ratio is markedly different in the $\Delta gppA$ mutant, the growth recovery profile of the mutant was similar to that of the WT strain (with an estimated recovery rate of $0.1941 \pm 0.0482 \text{ h}^{-2}$ for

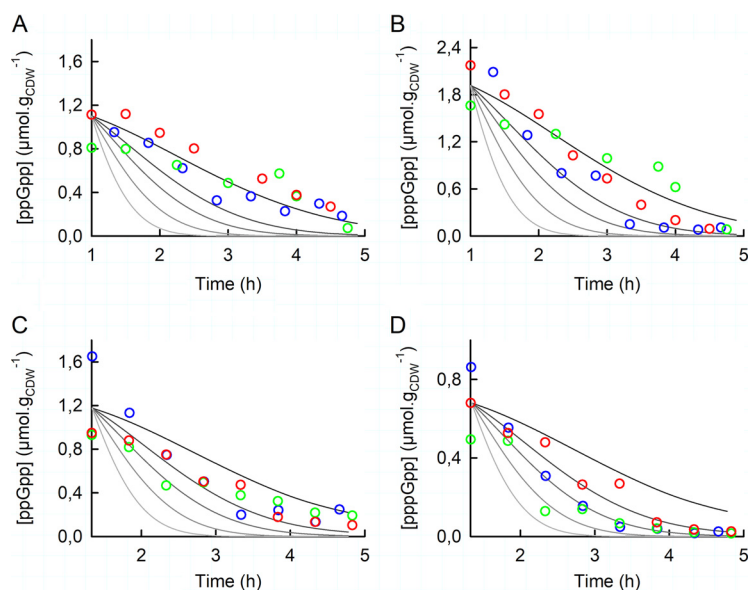


FIG 4 Dilution by growth of the intracellular concentrations of ppGpp and pppGpp for the $\Delta gppA$ mutant (A and B) and the WT strain (C and D) of *E. coli*. In all panels, the solid lines are the concentrations of (p)ppGpp calculated using the equation $d(p)ppGpp/dt = J_F - J_D - \mu_{(t)} \cdot (p)ppGpp$, where $(p)ppGpp$ is the amount of ppGpp or pppGpp; J_F and J_D are the fluxes of (p)ppGpp formation and degradation, respectively; and $\mu_{(t)}$ is the instantaneous growth rate. The black lines were calculated with $J_F = J_D$ and the gray lines were calculated with $(J_F - J_D) = a \cdot [\mu_{(t)} \cdot (p)ppGpp]$, with a ranging from 1 to 8, using as initial conditions the mean values of the (p)ppGpp concentrations and $\mu_{(t)}$ calculated from the three biological replicates of each strain. $\mu_{(t)}$ was calculated from the recovery rates determined for each strain, as listed in Table 1. Time zero on these graphs corresponds to the moment at which the ppGpp and pppGpp concentrations started to decline, i.e., 1 h after SHX addition for the $\Delta gppA$ mutant and 1 h 20 min after SHX addition for the WT. The mean values of the concentrations of ppGpp and pppGpp measured in three independent repeats (blue, green, and red) are plotted in panels A and B for the $\Delta gppA$ mutant and in panels C and D for the WT strain.

the $\Delta gppA$ mutant) (Fig. 3A and Table 1). This means that the buildup of pppGpp has no significant effect on growth recovery, with the only difference in this strain being slightly greater robustness (Table 1). Note that alanine and valine accumulated in the culture medium once again, as observed for the WT strain (Table S1).

The decrease in the (p)ppGpp concentration can be explained by growth. As described above for the WT and $\Delta gppA$ strains, the addition of SHX leads to the rapid accumulation of ppGpp and pppGpp (in a few minutes), a plateau stage that lasts for less than 1 h, and then a slow decrease of the concentrations of (p)ppGpp. It takes about 3 h in the latter phase for the intracellular concentrations of ppGpp and pppGpp to drop to the levels measured in the exponential phase (Fig. 2B). The question then arises as to whether the decrease in the concentration of (p)ppGpp is the result of an active degradation process or simply due to growth-driven dilution, as suggested by the ppGpp and pppGpp levels being correlated with growth during this phase. To answer this question, we first calculated what the intracellular concentrations of ppGpp and pppGpp would be if they were diluted only by growth. This would require that the formation fluxes of ppGpp (via RelA or GppA, for instance) be equal to its degradation fluxes (via SpoT, for instance) and, likewise, that the formation flux of pppGpp via RelA be equal to its degradation fluxes via GppA and SpoT. In the case of the $\Delta gppA$ mutant, the absence of GppA makes the situation easier to evaluate. In Fig. 4A and B, the solid black lines are the intracellular levels of ppGpp or pppGpp during the recovery phase considering growth dilution only. Because this line fits the measured intracellular concentrations of ppGpp and pppGpp relatively well, this means that the formation and degradation fluxes are equal and shows that in this strain, the decreases in ppGpp and pppGpp levels are mainly due to growth dilution rather than an active degradation

process. In contrast, the measured intracellular levels of ppGpp and pppGpp do not follow this line for the WT strain (Fig. 4C and D), meaning that a degradation process is involved. To estimate its contribution, we calculated what the intracellular ppGpp and pppGpp concentrations would be if the degradation flux were 1 to 8 times the growth dilution rate (Fig. 4, gray lines). For pppGpp (Fig. 4D), most of the experimental points are located between the first and the second gray lines, indicating that the degradation flux, likely via GppA, is about twice the growth dilution rate. The flux of ppGpp degradation is even more modest since the experimental points fall mostly between the black line and the first gray line (Fig. 4C). Altogether, these results indicate that the decrease in the concentration of (p)ppGpp is mostly accounted for by growth, even if GppA appears to participate somewhat in the degradation of pppGpp.

DISCUSSION

In this study, we investigated the dynamic response of *E. coli* to severe growth disruption and the role of the stringent response in this bacterium's ability to recover growth. With this aim, we monitored the growth and quantified consumed and excreted metabolites and intracellular levels of ppGpp and pppGpp in *E. coli* cultures before and after the addition of SHX.

The results demonstrate first that the K-12 WT strain of *E. coli* is resilient to SHX-induced growth disruption since its growth rate returned to pre-SHX levels a few hours after the perturbation. This recovery was first shown in the pioneering work of Tosa and Pizer (29), where growth inhibition was released by the addition of serine. In our work, *E. coli* appeared to recover growth by itself. Intriguingly, we observed that SHX disappeared rapidly from the medium and identified the cause as being a cell-related process, but it remains unclear whether SHX was degraded or simply internalized into the cells. The results of the experiment with the $\Delta relA$ mutant of *E. coli* K-12 indicate that resumption of growth is conditioned on the stringent response. Although just as with the WT, SHX disappeared from the medium, the $\Delta relA$ mutant failed to fully recover its pre-SHX growth rate, indicating that the stringent response is the major determinant of *E. coli*'s resilience to growth disruption. We also observed that this resilience is not affected by an overaccumulation of pppGpp. By eliminating GppA, we inverted the pppGpp/ppGpp concentration ratio, but the $\Delta gppA$ mutant's recovery from SHX addition was nevertheless similar to that of the WT. Although the robustness of the $\Delta gppA$ mutant was slightly greater, these results indicate that pppGpp does not play a significant role in growth recovery. This is in keeping with Mechold et al.'s conclusion that pppGpp is a less potent growth regulator than ppGpp (23).

The concentrations of both pppGpp and ppGpp peaked rapidly after the addition of SHX (in less than 10 min), which is in line with a previous study of a different bacterium (40). As mentioned above, in the WT strain, the concentrations of ppGpp were higher than those of pppGpp. This is in agreement with a previous report (24) and can be explained by the activity of RelA. In the absence of *gppA*, indeed, pppGpp was the dominant form in the first 2.5 h after SHX addition, as has also been reported by Mechold et al. (23). In line with these authors' interpretation (23), this suggests that RelA may favor the synthesis of pppGpp over ppGpp, while GppA adjusts the level of ppGpp. This also supports the argument that the principal pyrophosphate acceptor is GTP (11), which remains a matter of debate in the literature (41).

Our flux calculations show that the decrease in intracellular (p)ppGpp levels is mainly explained by growth-driven dilution during the recovery phase, meaning that the formation and degradation fluxes of (p)ppGpp are similar under this regime. One possibility might be that both RelA and SpoT are inactive. SpoT's hydrolase activity is indeed thought to be inhibited under physiological stress, notably in the presence of high levels of uncharged tRNA (15). It may be that the accumulation of ppGpp following the addition of SHX activates stress survival genes in an RpoS-dependent manner (27). Another possibility is that RelA and SpoT act at the same rate, with SpoT

continuously hydrolyzing the (p)ppGpp synthesized by RelA as a result of SHX exposure. Further experiments are required to unequivocally resolve these possibilities.

Our results also show that it is SHX itself that provokes growth arrest and that this growth arrest is associated with the excretion of alanine, valine, and, to a lesser extent, leucine. These three amino acids are derived from pyruvate and, along with glycine, are the most abundant amino acids in terms of biomass (42). Because this excretion is substantial and occurs after SHX addition, it can be interpreted as a (transient) metabolic overflow in response to a sudden drop in the demand for proteinogenic amino acids. However, further investigations are required to elucidate the regulatory mechanism underlying this metabolic overflow.

Concluding remarks. This report promotes a better understanding of the resilience of *E. coli* to severe growth disruption and the role of (p)ppGpp metabolism in this phenomenon. Our results and data, specifically the ppGpp and pppGpp concentrations, will hopefully serve as a hypothesis-generating resource for future studies on (p)ppGpp metabolism and more generally on the stringent response, a crucial process in bacterial adaptation and survival.

MATERIALS AND METHODS

Chemicals and reagents. DL-Serine hydroxamate (SHX) was purchased from Sigma-Aldrich (St. Quentin-Fallavier, France). LC-MS-grade solvents (methanol and acetonitrile) were obtained from Instrumentation Consommables et Service (ICS) (Lapeyrouse-Fossat, France).

Bacterial strains and growth conditions. All strains were derived from *E. coli* strain K-12 MG1655. The $\Delta relA$ and $\Delta gppA$ strains were constructed by P1 transduction of gene deletions marked with a kanamycin resistance cassette from the Keio collection (43). The kanamycin resistance cassette was removed using FLP recombinase from the pCP20 plasmid (44). All strains, plasmids, and primers are listed in Table S2 in the supplemental material, and the genetic modifications were checked by PCR.

Cells were cultured on M9-based synthetic minimal medium with the following composition per liter: 2.0 g KH_2PO_4 , 17.4 g $Na_2HPO_4 \cdot 12H_2O$, 0.5 g $MgSO_4$, 0.5 g NaCl, 2.0 g NH_4Cl , 0.1 g thiamine-HCl, and 1 ml of a trace element solution. The medium was supplemented with glucose. Glucose, thiamine, and $MgSO_4$ were sterilized by filtration (Minisart 0.2- μm syringe filter; Sartorius, Göttingen, Germany), and other solutions were autoclaved separately. $Na_2HPO_4 \cdot 12H_2O$ is not added to the medium for culture in bioreactors. All stock cultures were stored at $-80^\circ C$ in lysogeny broth (LB) medium containing glycerol (40%, vol/vol). For the cultures, 5 ml of cultures grown overnight in LB were used as the inoculum and then subcultured in shake flasks containing 50 ml of minimal medium with 3 g/liter glucose starting at an OD at 600 nm of 0.05 and incubated at $37^\circ C$ at 210 rpm for 15 h in an orbital shaker (Inova 4230; New Brunswick Scientific, New Brunswick, NJ, USA). Cells were harvested during the exponential growth phase by centrifugation for 10 min at $10,000 \times g$ at room temperature with a Sigma 3-18K centrifuge (Sigma-Aldrich, Seelze, Germany), washed with the same volume of fresh medium, and used to inoculate 500-ml bioreactors (Multifors; Infors HT, Bottmingen, Switzerland) containing 300 ml of minimal medium with 20 g/liter glucose (110 mM) at an OD at 600 nm of 0.15. The temperature was set to $37^\circ C$, and the pH was maintained at 7 by automatically adding 14% (g/g) ammonia or 11% (g/g) phosphoric acid. Aeration and the stirrer speed were controlled to maintain adequate aeration (dissolved oxygen tension [DOT] > 30% saturation). Cell growth was monitored by measuring the optical density at 600 nm with a Genesys 6 spectrophotometer (Thermo, Carlsbad, CA, USA). The percentages of O_2 , CO_2 , and N_2 were measured in the gas output during the culture process using a Dycor ProLine Process mass spectrometer (Ametek, Berwyn, PA, USA), and the data obtained were used to calculate the oxygen uptake rate (OUR) and the carbon dioxide evolution rate (CER). The stringent response was triggered by adding SHX at 0.8 mM to the culture when the OD reached 3.5.

Calculation of the instantaneous growth rate. The instantaneous growth rate [$\mu_{(t)}$] was determined by fitting the time evolution of the biomass concentration to (i) an exponential function prior to SHX addition and (ii) a parametric function after SHX addition, from which $\mu_{(t)}$ was calculated as $\mu_{(t)} = dX/(X \cdot dt)$.

Sampling and (p)ppGpp extraction. Culture medium (400 μl) was withdrawn from the bioreactor and vigorously mixed with 4.5 ml of a precooled acetonitrile-methanol- H_2O (4:4:2) solution at $-40^\circ C$ to rapidly quench metabolic activity (37). Immediately thereafter, 100 μl of ^{13}C -labeled metabolites was added to the latter mixture as an internal standard. The tubes were then placed in a cooling bath of ethanol precooled at $-40^\circ C$, evaporated to dryness in a SpeedVac (SC110A SpeedVac Plus; ThermoSavant, Waltham, MA, USA) under a vacuum for 4 h, and then stored at $-80^\circ C$ until needed.

IC-ESI-HRMS quantification of (p)ppGpp. ppGpp and pppGpp were quantified as described previously (37). Briefly, after resuspension of the cell extract samples in 20 mM ammonium acetate buffer at pH 9 to a final volume of 500 μl , cell debris was removed by centrifugation at $10,000 \times g$ for 10 min at $4^\circ C$. The samples were then analyzed using an ion chromatograph (IC; Thermo Scientific Dionex ICS-5000+ system; Dionex, Sunnyvale, CA, USA) coupled to an LTQ Orbitrap mass spectrometer (Thermo Fisher Scientific, Waltham, MA, USA) equipped with an electrospray ionization (ESI) probe. Mass spectrometry analysis was performed in the negative Fourier transform mass spectrometry mode at a

resolution of 30,000 (at m/z 400) in full-scan mode, with the following source parameters: a capillary temperature of 350°C, a source heater temperature of 300°C, a sheath gas flow rate of 50 AU (arbitrary units), an auxiliary gas flow rate of 5 AU, an S-lens RF level of 60%, and an ion spray voltage of 3.5 kV. The data were acquired using Xcalibur software (Thermo Fisher Scientific, Waltham, MA, USA). Three samples from three independent biological replicates were analyzed.

NMR analysis of culture supernatants. Extracellular metabolites were identified and quantified by nuclear magnetic resonance (NMR). Broth samples were collected at different times and filtered (Minisart 0.2- μ m syringe filter; Sartorius, Göttingen, Germany). The supernatants, consisting of the culture medium, were mixed with 100 μ l of D₂O with 2.35 g/liter of TSP-d4 (deuterated trimethylsilylpropionic acid) as an internal reference. Proton NMR spectra were recorded on an Avance III 800-MHz spectrometer equipped with a 5 mM QCI-P cryoprobe (Bruker, Rheinstatten, Germany). Quantitative ¹H NMR was performed at 280 K, using a 30° pulse and a relaxation delay of 10 s. Two-dimensional ¹H-¹³C heteronuclear single quantum coherence (HSQC) spectra were recorded at 280 K to quantify SHX in the supernatant. Sixteen scans were acquired with 4,096 by 128 datapoints and 13.35- by 60-ppm spectral widths. The spectra were processed and the metabolites were quantified using Topspin 3.1 (Bruker, Rheinstatten, Germany). Extracellular metabolites from three independent biological replicates were analyzed.

SUPPLEMENTAL MATERIAL

Supplemental material is available online only.

FIG S1, TIF file, 2.7 MB.

FIG S2, TIF file, 0.3 MB.

FIG S3, TIF file, 3.4 MB.

FIG S4, TIF file, 0.6 MB.

FIG S5, TIF file, 3.2 MB.

FIG S6, TIF file, 3.3 MB.

TABLE S1, DOCX file, 0.02 MB.

TABLE S2, DOCX file, 0.02 MB.

DATA SET S1, XLSX file, 0.1 MB.

ACKNOWLEDGMENTS

We gratefully acknowledge financial support from the Bioprocess R&D department of Sanofi Pasteur and the Association Nationale de la Technologie (ANRT).

We thank MetaToul (Metabolomics and Fluxomics Facilities, Toulouse, France [www.metatoul.fr]) and its staff for technical support and access to NMR and mass spectrometry facilities. MetaToul is part of the French National Infrastructure for Metabolomics and Fluxomics (www.metabohub.fr), funded by the ANR (MetaboHUB-ANR-11-INBS-0010).

REFERENCES

- Vadia S, Levin PA. 2015. Growth rate and cell size: a re-examination of the growth law. *Curr Opin Microbiol* 24:96–103. <https://doi.org/10.1016/j.mib.2015.01.011>.
- Kanjee U, Ogata K, Houry WA. 2012. Direct binding targets of the stringent response alarmone (p)ppGpp. *Mol Microbiol* 85:1029–1043. <https://doi.org/10.1111/j.1365-2958.2012.08177.x>.
- Potrykus K, Cashel M. 2008. (p)ppGpp: still magical? *Annu Rev Microbiol* 62:35–51. <https://doi.org/10.1146/annurev.micro.62.081307.162903>.
- Srivatsan A, Wang JD. 2008. Control of bacterial transcription, translation and replication by (p)ppGpp. *Curr Opin Microbiol* 11:100–105. <https://doi.org/10.1016/j.mib.2008.02.001>.
- Hüttener M, Prieto A, Espelt J, Bernabeu M, Juárez A. 2018. Stringent response and AggR-dependent virulence regulation in the enteroaggregative *Escherichia coli* strain 042. *Front Microbiol* 9:717. <https://doi.org/10.3389/fmicb.2018.00717>.
- Geiger T, Francois P, Liebeke M, Fraunholz M, Goerke C, Krismer B, Schrenzel J, Lalk M, Wolz C. 2012. The stringent response of *Staphylococcus aureus* and its impact on survival after phagocytosis through the induction of intracellular PSMs expression. *PLoS Pathog* 8:e1003016. <https://doi.org/10.1371/journal.ppat.1003016>.
- Wu N, He L, Cui P, Wang W, Yuan Y, Liu S, Xu T, Zhang S, Wu J, Zhang W, Zhang Y. 2015. Ranking of persister genes in the same *Escherichia coli* genetic background demonstrates varying importance of individual persister genes in tolerance to different antibiotics. *Front Microbiol* 6:1003. <https://doi.org/10.3389/fmicb.2015.01003>.
- Verstraeten N, Knapien WJ, Kint CI, Liebens V, Van den Bergh B, Dewachter L, Michiels JE, Fu Q, David CC, Fierro AC, Marchal K, Beirlant J, Versées W, Hofkens J, Jansen M, Fauvart M, Michiels J. 2015. Opg and membrane depolarization are part of a microbial bet-hedging strategy that leads to antibiotic tolerance. *Mol Cell* 59:9–21. <https://doi.org/10.1016/j.molcel.2015.05.011>.
- Piskunova J, Maisonneuve E, Germain E, Gerdes K, Severinov K. 2017. Peptide-nucleotide antibiotic microcin C is a potent inducer of stringent response and persistence in both sensitive and producing cells. *Mol Microbiol* 104:463–471. <https://doi.org/10.1111/mmi.13640>.
- Atkinson GC, Tenson T, Haurlyuk V. 2011. The RelA/SpoT homolog (RSH) superfamily: distribution and functional evolution of ppGpp synthetases and hydrolases across the Tree of Life. *PLoS One* 6:e23479. <https://doi.org/10.1371/journal.pone.0023479>.
- Cashel M, Gentry D, Hernandez VJ, Vinella D. 1996. The stringent response, p 1458–1496. *In* Neidhardt FC, Curtiss R, III, Ingraham JL, Lin ECC, Low KB, Magasanik B, Reznikoff WS, Riley M, Schaechter M, Umberger HE (ed), *Escherichia coli and Salmonella: cellular and molecular biology*, 2nd ed, vol 1. ASM Press, Washington, DC.
- Haseltine WA, Block R. 1973. Synthesis of guanosine tetra- and penta-phosphate requires the presence of a codon-specific, uncharged transfer ribonucleic acid in the acceptor site of ribosomes. *Proc Natl Acad Sci U S A* 70:1564–1568. <https://doi.org/10.1073/pnas.70.5.1564>.
- Wendrich TM, Blaha G, Wilson DN, Marahiel MA, Nierhaus KH. 2002. Dissection of the mechanism for the stringent factor RelA. *Mol Cell* 10:779–788. [https://doi.org/10.1016/s1097-2765\(02\)00656-1](https://doi.org/10.1016/s1097-2765(02)00656-1).
- Battesti A, Bouveret E. 2006. Acyl carrier protein/SpoT interaction, the switch

- linking SpoT-dependent stress response to fatty acid metabolism. *Mol Microbiol* 62:1048–1063. <https://doi.org/10.1111/j.1365-2958.2006.05442.x>.
15. Murray KD, Bremer H. 1996. Control of spoT-dependent ppGpp synthesis and degradation in *Escherichia coli*. *J Mol Biol* 259:41–57. <https://doi.org/10.1006/jmbi.1996.0300>.
 16. Spira B, Silberstein N, Yagil E. 1995. Guanosine 3',5'-bispyrophosphate (ppGpp) synthesis in cells of *Escherichia coli* starved for Pi. *J Bacteriol* 177:4053–4058. <https://doi.org/10.1128/jb.177.14.4053-4058.1995>.
 17. Bougdour A, Gottesman S. 2007. ppGpp regulation of RpoS degradation via anti-adaptor protein IraP. *Proc Natl Acad Sci U S A* 104:12896–12901. <https://doi.org/10.1073/pnas.0705561104>.
 18. Vinella D, Albrecht C, Cashel M, D'Ari R. 2005. Iron limitation induces SpoT-dependent accumulation of ppGpp in *Escherichia coli*. *Mol Microbiol* 56:958–970. <https://doi.org/10.1111/j.1365-2958.2005.04601.x>.
 19. Fernández-Coll L, Cashel M. 2018. Contributions of SpoT hydrolase, SpoT synthetase, and RelA synthetase to carbon source diauxic growth transitions in *Escherichia coli*. *Front Microbiol* 9:1802. <https://doi.org/10.3389/fmicb.2018.01802>.
 20. English BP, Haurlyuk V, Sanamrad A, Tankov S, Dekker NH, Elf J. 2011. Single-molecule investigations of the stringent response machinery in living bacterial cells. *Proc Natl Acad Sci U S A* 108:E365–E373. <https://doi.org/10.1073/pnas.1102255108>.
 21. Zhang Y, Zborníková E, Rejman D, Gerdes K. 2018. Novel (p)ppGpp binding and metabolizing proteins of *Escherichia coli*. *mBio* 9:e02188-17. <https://doi.org/10.1128/mBio.02188-17>.
 22. Wang B, Grant RA, Laub MT. 2020. ppGpp coordinates nucleotide and amino-acid synthesis in *E. coli* during starvation. *Mol Cell* 80:29–42.e10. <https://doi.org/10.1016/j.molcel.2020.08.005>.
 23. Mechold U, Potrykus K, Murphy H, Murakami KS, Cashel M. 2013. Differential regulation by ppGpp versus pppGpp in *Escherichia coli*. *Nucleic Acids Res* 41:6175–6189. <https://doi.org/10.1093/nar/gkt302>.
 24. Denapoli J, Tehranchi AK, Wang JD. 2013. Dose-dependent reduction of replication elongation rate by (p)ppGpp in *Escherichia coli* and *Bacillus subtilis*. *Mol Microbiol* 88:93–104. <https://doi.org/10.1111/mmi.12172>.
 25. Zhu M, Dai X. 2019. Growth suppression by altered (p)ppGpp levels results from non-optimal resource allocation in *Escherichia coli*. *Nucleic Acids Res* 47:4684–4693. <https://doi.org/10.1093/nar/gkz211>.
 26. Durfee T, Hansen A-M, Zhi H, Blattner FR, Jin DJ. 2008. Transcription profiling of the stringent response in *Escherichia coli*. *J Bacteriol* 190:1084–1096. <https://doi.org/10.1128/JB.01092-07>.
 27. Traxler MF, Summers SM, Nguyen H-T, Zacharia VM, Hightower GA, Smith JT, Conway T. 2008. The global, ppGpp-mediated stringent response to amino acid starvation in *Escherichia coli*. *Mol Microbiol* 68:1128–1148. <https://doi.org/10.1111/j.1365-2958.2008.06229.x>.
 28. Svitil AL, Cashel M, Zyskind JW. 1993. Guanosine tetraphosphate inhibits protein synthesis in vivo. A possible protective mechanism for starvation stress in *Escherichia coli*. *J Biol Chem* 268:2307–2311.
 29. Tosa T, Pizer LI. 1971. Effect of serine hydroxamate on the growth of *Escherichia coli*. *J Bacteriol* 106:966–971. <https://doi.org/10.1128/JB.106.3.966-971.1971>.
 30. Ross W, Sanchez-Vazquez P, Chen AY, Lee J-H, Burgos HL, Gourse RL. 2016. ppGpp binding to a site at the RNAP-DksA interface accounts for its dramatic effects on transcription initiation during the stringent response. *Mol Cell* 62:811–823. <https://doi.org/10.1016/j.molcel.2016.04.029>.
 31. Weygand-Durasević I, Ban N, Jahn D, Söll D. 1993. Yeast seryl-tRNA synthetase expressed in *Escherichia coli* recognizes bacterial serine-specific tRNAs in vivo. *Eur J Biochem* 214:869–877. <https://doi.org/10.1111/j.1432-1033.1993.tb17990.x>.
 32. Pizer LI, Merlie JP. 1973. Effect of serine hydroxamate on phospholipid synthesis in *Escherichia coli*. *J Bacteriol* 114:980–987. <https://doi.org/10.1128/JB.114.3.980-987.1973>.
 33. Marisch K, Bayer K, Scharl T, Mairhofer J, Krempel PM, Hummel K, Razzazi-Fazeli E, Striedner G. 2013. A comparative analysis of industrial *Escherichia coli* K-12 and B strains in high-glucose batch cultivations on process-, transcriptome- and proteome level. *PLoS One* 8:e70516. <https://doi.org/10.1371/journal.pone.0070516>.
 34. Enjalbert B, Letisse F, Portais J-C. 2013. Physiological and molecular timing of the glucose to acetate transition in *Escherichia coli*. *Metabolites* 3:820–837. <https://doi.org/10.3390/metabo3030820>.
 35. Yodo N, Wang P. 2016. Resilience allocation for early stage design of complex engineered systems. *J Mech Des* 138:091402. <https://doi.org/10.1115/1.4033990>.
 36. Carvalho G, Forestier C, Mathias J-D. 2019. Antibiotic resilience: a necessary concept to complement antibiotic resistance? *Proc Biol Sci* 286:20192408. <https://doi.org/10.1098/rspb.2019.2408>.
 37. Patacq C, Chaudet N, Létisse F. 2018. Absolute quantification of ppGpp and pppGpp by double-spike isotope dilution ion chromatography-high-resolution mass spectrometry. *Anal Chem* 90:10715–10723. <https://doi.org/10.1021/acs.analchem.8b00829>.
 38. Samarrai W, Liu DX, White A-M, Studamire B, Edelstein J, Srivastava A, Widom RL, Rudner R. 2011. Differential responses of *Bacillus subtilis* rRNA promoters to nutritional stress. *J Bacteriol* 193:723–733. <https://doi.org/10.1128/JB.00708-10>.
 39. Somerville CR, Ahmed A. 1979. Mutants of *Escherichia coli* defective in the degradation of guanosine 5'-triphosphate, 3'-diphosphate (pppGpp). *Mol Gen Genet* 169:315–323. <https://doi.org/10.1007/BF00382277>.
 40. Riesenberger D, Bergter F, Kari C. 1984. Effect of serine hydroxamate and methyl alpha-D-glucopyranoside treatment on nucleoside polyphosphate pools, RNA and protein accumulation in *Streptomyces hygroscopicus*. *J Gen Microbiol* 130:2549–2558. <https://doi.org/10.1099/00221287-130-10-2549>.
 41. Sajish M, Kalayil S, Verma SK, Nandicoori VK, Prakash B. 2009. The significance of EXDD and RXKD motif conservation in Rel proteins. *J Biol Chem* 284:9115–9123. <https://doi.org/10.1074/jbc.M807187200>.
 42. Feist AM, Herrgård MJ, Thiele I, Reed JL, Palsson BØ. 2009. Reconstruction of biochemical networks in microorganisms. *Nat Rev Microbiol* 7:129–143. <https://doi.org/10.1038/nrmicro1949>.
 43. Baba T, Ara T, Hasegawa M, Takai Y, Okumura Y, Baba M, Datsenko KA, Tomita M, Wanner BL, Mori H. 2006. Construction of *Escherichia coli* K-12 in-frame, single-gene knockout mutants: the Keio collection. *Mol Syst Biol* 2:2006.0008. <https://doi.org/10.1038/msb4100050>.
 44. Cherepanov PP, Wackernagel W. 1995. Gene disruption in *Escherichia coli*: TcR and KmR cassettes with the option of Flp-catalyzed excision of the antibiotic-resistance determinant. *Gene* 158:9–14. [https://doi.org/10.1016/0378-1119\(95\)00193-a](https://doi.org/10.1016/0378-1119(95)00193-a).